NOAA-20 VISIBLE INFRARED IMAGING RADIOMETER SUITE (VIIRS) DAY-NIGHT BAND CALIBRATION USING THE SCHEDULED LUNAR COLLECTIONS

Taeyoung Choi[1,2], Changyong Cao[2] , Xi Shao[2,3]

[1]Global Science and Technology, [2]NOAA Center for Satellite Applications and Research (STAR), [3]University of Maryland College Park.

ABSTRACT

As a panchromatic band, the Day-Night Band (DNB) on National Oceanic Atmospheric Administration (NOAA)-20 Visible Infrared Imaging Radiometer Suite (VIIRS) has a unique capability of observing very low radiances down to Nano-watt [cm^{-2} sr^{-1}] level, because of its three different focal planes with gain stages. The DNB radiometric calibration is based on the Solar Diffuser observations near the night to day time termination points. Besides the primary calibration source of SD, the moon provides alternative source of calibration with a specific lunar roll maneuvers. This study provides detailed methodology and results of lunar calibration for NOAA-20 VIIRS sensor and initial two year DNB radiometric calibration results from SD and scheduled lunar calibration. Over two years of NOAA-20 VIIRS operation, the Low Gain Stage (LGS) slope (inverse gain) trend showed a decreasing trend, whereas the calculated monthly lunar F-factor showed a stable response (inverse gain normalized to the lunar irradiance model) using a lunar irradiance model. These differences are monitored, compared, and applied for the best quality of NOAA-20 VIIRS DNB product.

Index Terms— NOAA-20, VIIRS, SDR, Day-Night Band, DNB, Moon, RSB

1. INTRODUCTION

On November 18, 2017, the National Oceanic Atmospheric Administration (NOAA)-20 was launched following the predecessor Suomi National Polar-orbiting Partnership (S-NPP) satellite. The two satellites including Visible Infrared Imaging Radiometer Suite (VIIRS) sensors and they provide entire Earth observations once per day with a wide field-of-view (FOV) of 112.56 degrees through the day-night band (DNB), Reflective Solar Bands (RSBs) and Thermal Emissive Bands (TEBs) covering a spectral range of 0.4 to 12.5μm at a nominal altitude of 829 km [1-3]. Compared to NASA's historical Terra and Aqua Moderate Resolution Imaging Spectroradiometer (MODIS) sensors, VIIRS has a unique DNB with a low-level light sensor (LLLS) of detecting visible radiation at night with controlled growth in spatial resolution through use of segmented detectors and rotation of the ground instantaneous field of view (GIFOV) from the Operational Linescan System (OLS) [4]. The dynamic range of the DNB is from 3.0×10^{-9} cm^{-2} sr^{-1} to 2.0×10^{-2} cm^{-2} sr^{-1} radiance levels. The radiometric calibration uncertainty requirements are varying from 100 percent at minimum radiance level to 5 percent in LGS at half of the maximum radiance level. The S-NPP on-orbit DNB minimum detectable radiance was approximately 2.0×10^{-10} cm^{-2} sr^{-1} level [5]. This extreme light detection sensitivity opened up a new field of nighttime remote sensing study such as generating nighttime light products by NOAA [6], boat identification [7], and social and economic activity estimations [8, 9].

Even though the high uncertainty requirement at minimum radiance level, an accurate DNB calibration is required to improve the quality of low-light detection. One of the key parameter is the DNB dark offset because any remaining errors will be propagated the calibration gain estimation which also affects to the calibrated radiance. The regular dark offsets are easily estimated by the dark Space View (SV) observations for RSB and TEB calibrations packaged in the On-Board Calibrator (OBC) as a Sensor Data Record (SDR) products. The DNB LGS slopes (or inverse gain) are derived by the offset corrected SD Digital Number (DN) by the SV observations. The OBC data file only provide one aggregation zone information per scan out of 32 aggregation zones [10, 11]. Unlike OBC data file, the EV DNB data from the VIIRS Recommended Operating Procedure (VROP) collections during the new moon over the pacific ocean can estimate the dark offset in all the aggregation zones and in all the gain stages [11].

This paper is focused on the NOAA-20 VIIRS DNB calibration using the scheduled lunar collections over the last two years. This paper provides an algorithm descriptions of DNB lunar calibration as an alternative calibration source. Using a lunar irradiance model called Global Space-based Inter-Calibration System (GSICS) Implementation of ROLO (GIRO), the DNB lunar F-factors (inverse gain normalized by GIRO) were calculated and compared to the SD LGS slope trends. An increasing differences were found between the lunar F-factor and DNB LGS gain trend. Similar results were observed in the short wavelength RSB band (M1~M4) calibration results from a previous study [12]. Following the RSB case, the operational LGS gains were delivered in April

2018 and still remained to be in constant levels in the NOAA-20 VIIRS SDR operational production.

2. NOAA-20 VIIRS SCHEDULED LUNAR CALIBRATION

The monthly lunar calibrations require lunar roll maneuver predictions to view the moon at the center of the SV port. With a specific spacecraft roll angle, VIIRS views the moon through the SV port with a specific phase angle near -51 degrees. The negative sign of the phase angle means that the moon is in the waxing lunar phase. The detailed procedures of the determining the monthly roll maneuver is well documented in the Wilson's study [13]. When performing the lunar roll maneuver and collection, the sector rotation commend needs to be uploaded to the instrument to locate the moon in the desired location of the EV frame as shown in Figure 1. Table 1 provides date and times of all the scheduled lunar collections since launch except the first one on December 29, 2017. No DNB data was available with the first collection because the DNB focal plane temperatures was not cooled-down to the operational range.

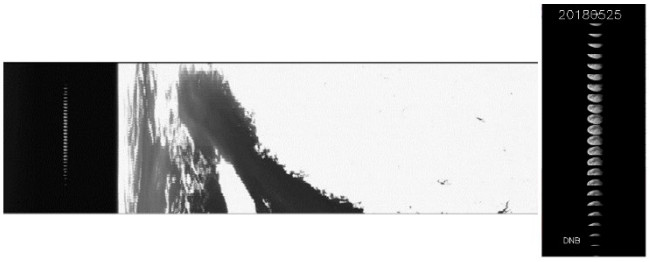

Figure 1. NOAA-20 VIIRS scheduled lunar collection on 2018-5-25. A sector rotation commend was applied at the time of the lunar collection to locate the center of the moon in the desired EV frame.

Table 1. NOAA-20 VIIRS scheduled lunar collections.

Date	Center Time [UTC]	Phase angle
1/27/2018	19:22:49	-51.34
2/26/2018	04:47:03	-51.13
3/27/2018	12:32:59	-51.16
4/25/2018	20:21:36	-50.98
5/25/2018	05:53:34	-50.31
6/23/2018*	13:43:07	-51.42
11/19/2018	1:54:40	-50.99
12/18/2018	17:56:34	-51.32
1/17/2019	9:59:00	-50.81
2/15/2019	22:44:36	-50.84
3/17/2019	8:11:00	-51.19
4/15/2019	15:59:05	-51.02
5/14/2019	22:07:57	-50.91
6/13/2019*	04:17:15	-50.87
11/7/2019*	23:37:25	-51.00
12/7/2019	19:03:36	-51.01

* No roll maneuver was required.

2. METHDOLOGY

At the time of the lunar collection, the lunar irradiance can be predicted using a lunar irradiance model called GIRO. The GIRO model was developed by European Organization for the Exploitation of Meteorological Satellites (EUMETSAT) in collaboration with the international GSICS community members based on USGS ROLO (http://gsics.atmos.umd.edu/bin/view/Development/LunarWorkArea). The DNB lunar F-factors are calculated by Equation 1.

$$F_{Lunar}(t) = \frac{I_{GIRO}(t)}{I_{VIIRS\_Observed}(t)} \quad (1)$$

The observed lunar irradiance, $I_{VIIRS\_Observed}(t)$, is derived from the mean radiance of the moon over all the effective moon pixel with solid angle and phase angle correction part as shown in Equation 2.

$$I_{VIIRS\_Observed}(t) = \frac{\pi \cdot R_{moon}^2}{D_{Sat\_Moon}^2} \cdot \frac{1+\cos(\emptyset)}{2} \cdot \sum_{Pixel} \frac{L_{Pixel}}{N} \quad (2)$$

In Equation 2, the portion of the effective area of the moon by the phase angle is derived by the lunar phase angle ($\emptyset$). The lunar F-factor calculation methodology is the same as RSB case and the detailed descriptions are reported in our previous studies [14, 15].

The DNB LGS slope (inverse gain) is calculated in Equation 3 by using the 14 or 15 SD observations per day near the night to daytime termination point.

$$Slope(h,d,Ag) = \frac{cos\theta_{SD} RVS_{SD} \frac{\int \frac{\Phi_{Sun}(\lambda)}{4\pi d^2} \tau_{SD} BRDF(\lambda) H(t) d\lambda}{\int RSR d\lambda}}{dn_{SD}(h,d,Ag)} \quad (3)$$

In Equation 3, the incident angle to the SD screen is corrected by cosine of solar angle (θ_{SD}), RVS is response versus scan at SD angle on to the Half-Angle Mirror (HAM), the in-coming solar flux at a given wavelength is $\Phi_{Sun}(\lambda)$, d is Sun to VIIRS distance, SD screen vignetting function is τ_{SD}, BRDF is Bi-directional Reflectance Distribution Function of the SD, $H(t)$ is SD degradation at the time of lunar observation, RSR is the Relative Spectral Response of DNB, and dn_{SD} is bias removed SD DN using the corresponding SV observation in the same scan. Slopes were calculated in each ham (h), detector (d), and aggregation zone (Ag) independently. The calculated slope values are the primary radiometric coefficients for DNB calibration. The time-dependent trend of the slope values will be compared to the lunar F-factors as a part of verification and validation process.

2. RESULTS

During the lunar roll maneuvers, the sector rotation command was activated and applied for about 5 minutes centered at the center time listed in Table 1. The official DNB SDR granules does not include valid EV data, since it was populated with a fill-value during the sector rotation. To get the lunar observations, the RDR granules were downloaded around the center collection time. The raw DN counts in the DNB RDR granules need to be convert to a normal DN value, since upper last 2 digits (15th and 16th digits) were assigned for gain state recognition. In other words, the raw RDR EV observation pixels must be converted to 14 bit value by removing the gain state bits. These gain states for each pixel is automatically selected by on-orbit algorithm. Figure 2 shows the three gain states around the moon with multiple scans of the moon. The white color near the center of the moon represents LGS, the gray color around the moon is MGS, and the black color indicates HGS.

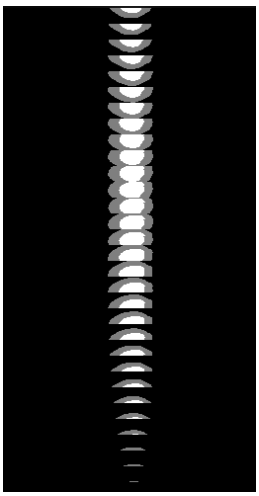

Figure 2. Retrieved gain state information with the scheduled lunar collection on 1/17/2019 at 09:57:30 UTC.

Because of the on-board automatic gain selection algorithm, the LGS detector offset at zero signal could not be estimated within the deep space view near the moon. The gain state in the deep space was selected to be in the HGS as shown Figure 2. To determine the LGS detector offset of a specific scheduled lunar collection, the previous operational DN0 LUT was applied on each frame, ham side and detector. For example, when a scheduled lunar collection on 1/27/2018 was processed, the DN0 LUT was used to correct the detector offset from the corresponding new moon VROP collection on 1/17/2018. Actually all the lunar collections were acquired in the DNB aggregation zone 21.

As seen in Figures 1 and 2, the size of the moon was slightly larger than a scan size, because of the sub-pixel aggregation in the zone 21. A reconstruction process was necessary before proceeding any further calculation. After removing the gain information, the center scan was found in each scheduled lunar collection. Additional lines of moon scans were found using the scans away from the center. When the full moon image was reconstructed, there were extra 2 rows were added and the final full moon size became 18 lines in the track direction, whereas a scan is consist with 16 lines from the 16 aggregated detectors.

Figure 4 shows the normalized DNB lunar F-factors after taking ratios between the GIRO and observed irradiances. The lunar F-factors were quite stable with small variations.

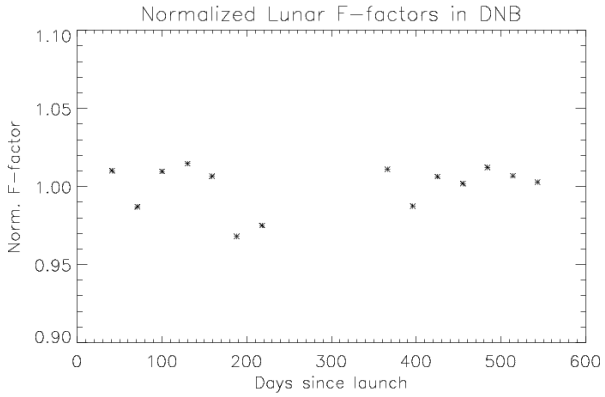

Figure 3. NOAA-20 VIIRS normalized DNB Lunar F-factors.

After normalization, the lunar F-factors are roughly within ±3% range. The corresponding primary SD slopes are calculated by using Equation 3 in Figure 4. To be able to compare with the lunar F-factors, the SD slope were also normalized. The SD LGS slope change over the period is about 0.7% level, whereas the lunar F-factors show stable response. These differences are very similar to the RSB case [12].

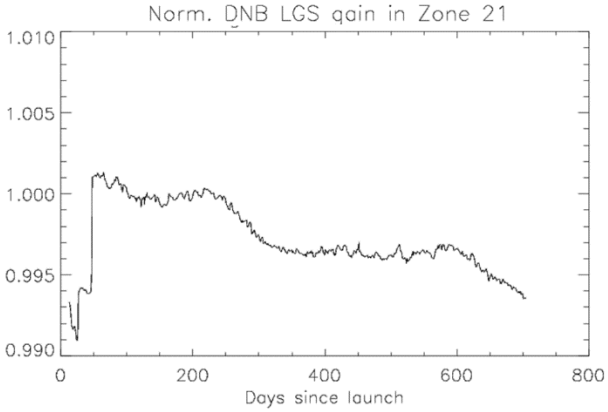

Figure 4. NOAA-20 VIIRS DNB normalized LGS slope in aggregation zone 21.

4. SUMMARY

As a key sensor radiometric parameter, the NOAA-20 VIIRS lunar F-factors has been calculated and monitored on-orbit for DNB with the regularly scheduled lunar calibration. The initial lunar F-factors have remained stable within ±0.3 percent level, whereas the SD based slope values have been reduced approximately 0.7 percent since launch. This results are very similar to the RSB calibration comparisons between

the SD and lunar F-factors especially for the short wavelength bands. NOAA VIIRS SDR team is continuously monitoring DNB SD slope and lunar F-factor trends to make sure for the best radiometric calibration practices for the users.

5. ACKNOWLEDGMENT

Authors thank to EUMETSAT for sharing the GIRO (version 1.0) with the NOAA VIIRS team. The paper contents are solely the opinions of the authors and do not constitute a statement of policy, decision, or position on behalf of NOAA or the U.S. government. This work is funded by the NOAA JPSS program.

6. REFERENCE

[1] C. Cao *et al.*, "NOAA Technical Report NESDIS 142 Visible Infrared Imaging Radiometer Suite (VIIRS) Sensor Data Record (SDR) User ' s Guide," Sep. 10, 2013 2013.

[2] C. Cao *et al.*, "Suomi NPP VIIRS sensor data record verification, validation, and long-term performance monitoring," *Journal of Geophysical Research: Atmospheres,* vol. 118, no. 20, pp. 11,664-11,678, 2013.

[3] C. Cao, F. J. De Luccia, X. Xiong, R. Wolfe, and F. Weng, "Early On-Orbit Performance of the Visible Infrared Imaging Radiometer Suite Onboard the Suomi National Polar-Orbiting Partnership (S-NPP) Satellite," *IEEE Transactions on Geoscience and Remote Sensing,* vol. 52, no. 2, pp. 1142-1156, 2014.

[4] N. Baker and H. Kilcoyne, "Joint Polar Satellite System (JPSS) VIIRS Radiometric Calibration Algorithm Theoretical Basis Document (ATBD)," J. P. S. S. J. G. Project, Ed., ed. NOAA and NASA: NOAA & NASA, 2011.

[5] L. B. Liao, S. Weiss, S. Mills, and B. Hauss, "Suomi NPP VIIRS day-night band on-orbit performance," *Journal of Geophysical Research: Atmospheres,* vol. 118, no. 22, pp. 12,705-12,718, 2013.

[6] C. D. Elvidge, K. Baugh, M. Zhizhin, F. C. Hsu, and T. Ghosh, "VIIRS night-time lights," *International Journal of Remote Sensing,* vol. 38, no. 21, pp. 5860-5879, 2017.

[7] C. Elvidge, M. Zhizhin, K. Baugh, and F.-C. Hsu, "Automatic Boat Identification System for VIIRS Low Light Imaging Data," *Remote Sensing,* vol. 7, no. 3, pp. 3020-3036, 2015.

[8] N. Zhao, F.-C. Hsu, G. Cao, and E. L. Samson, "Improving accuracy of economic estimations with VIIRS DNB image products," *International Journal of Remote Sensing,* vol. 38, no. 21, pp. 5899-5918, 2017/11/02 2017.

[9] C. Cao, X. Shao, and S. Uprety, "Detecting Light Outages After Severe Storms Using the S-NPP/VIIRS Day/Night Band Radiances," *IEEE Geoscience and Remote Sensing Letters,* vol. 10, no. 6, pp. 1582-1586, 2013.

[10] S. Lee, K. Chiang, X. Xiong, C. Sun, and S. Anderson, "The S-NPP VIIRS Day-Night Band On-Orbit Calibration/Characterization and Current State of SDR Products," *Remote Sensing,* vol. 6, no. 12, pp. 12427-12446, 2014.

[11] Y. Gu, S. Uprety, S. Blonski, B. Zhang, and C. Cao, "Improved algorithm for determining the Visible Infrared Imaging Radiometer Suite Day/Night Band high-gain stage dark offset free from light contamination," *Appl Opt,* vol. 58, no. 6, pp. 1400-1407, Feb 20 2019.

[12] T. Choi, X. Shao, S. Blonski, W. Wang, S. Uprety, and C. Cao, "NOAA-20 VIIRS initial on-orbit radiometric calibration using scheduled lunar observations," presented at the Earth Observing Systems XXIV, 2019.

[13] T. Wilson and X. Xiong, "Planning lunar observations for satellite missions in low-Earth orbit," *Journal of Applied Remote Sensing,* vol. 13, no. 02, 2019.

[14] T. Choi, X. Shao, and C. Cao, "On-orbit radiometric calibration of Suomi NPP VIIRS reflective solar bands using the Moon and solar diffuser," *Appl Opt,* vol. 57, no. 32, pp. 9533-9542, Nov 10 2018.

[15] T. Choi, X. Shao, C. Cao, and F. Weng, "Radiometric Stability Monitoring of the Suomi NPP Visible Infrared Imaging Radiometer Suite (VIIRS) Reflective Solar Bands Using the Moon," *Remote Sensing,* vol. 8, no. 1, 2015.